Mechanism, Mutagenesis, and Chemical Rescue of a β-Mannosidase from *Cellulomonas fimi*†

David L. Zechel,‡ Stephen P. Reid,‡ Dominik Stoll,§ Oyekanmi Nashiru,§ R. Antony J. Warren,§ and Stephen G. Withers*,‡

PENCE and Departments of Chemistry and Microbiology, University of British Columbia, Vancouver, British Columbia, Canada V6T 1Z1

Received February 27, 2003; Revised Manuscript Received April 28, 2003

ABSTRACT: The chemical mechanism of a retaining β-mannosidase from *Cellulomonas fimi* has been characterized through steady-state kinetic analyses with a range of substrates, coupled with chemical rescue studies on both the wild-type enzyme and mutants in which active site carboxyl groups have been replaced. Studies with a series of aryl β-mannosides of vastly different reactivities ($pK_a^{lg} = 4-10$) allowed kinetic isolation of the glycosylation and deglycosylation steps. Substrate inhibition was observed for all but the least reactive of these substrates. Brønsted analysis of k_{cat} revealed a downward breaking plot ($\beta_{lg} = -0.54 \pm 0.05$) that is consistent with a change in rate-determining step (glycosylation to deglycosylation), and this was confirmed by partitioning studies with ethylene glycol. The pH dependence of k_{cat}/K_m follows an apparent single ionization of a group of $pK_a = 7.65$ that must be protonated for catalysis. The tentative assignment of E429 as the acid−base catalyst of Man2A on the basis of sequence alignments with other family 2 glycosidases was confirmed by the increased turnover rate observed for the mutant E429A in the presence of azide and fluoride, leading to the production of β-mannosyl azide and β-mannosyl fluoride, respectively. A pH-dependent chemical rescue of E429A activity is also observed with citrate. Substantial oxocarbenium ion character at the transition state was demonstrated by the α-deuterium kinetic isotope effect for Man2A E429A of $\alpha\text{-}D^{(V)} = 1.12 \pm 0.01$. Surprisingly, this isotope effect was substantially greater in the presence of azide ($\alpha\text{-}D^{(V)} = 1.166 \pm 0.009$). Likely involvement of acid/base catalysis was revealed by the pH dependence of k_{cat} for Man2A E429A, which follows a bell-shaped profile described by pK_a values of 6.1 and 8.4, substantially different from that of the wild-type enzyme. The glycosidic bond cleaving activity of Man2A E519A and E519S nucleophile mutants is restored with azide and fluoride and appears to correlate with the corresponding "glycosynthase" activities. The contribution of the substrate 2-hydroxyl to stabilization of the Man2A glycosylation transition state ($\Delta\Delta G^{\ddagger} = 5.1$ kcal mol^{-1}) was probed using a 2-deoxymannose substrate. This value, surprisingly, is comparable to that found from equivalent studies with β-glucosidases despite the geometric differences at C-2 and the importance of hydrogen bonding at that position. Modes of stabilizing the mannosidase transition state are discussed.

A significant component of enzymatic catalysis is derived from noncovalent enzyme−substrate interactions that are optimized in the transition state. Therefore, to understand enzyme catalysis, it is important to quantify contributions from this source. Good enzyme systems for such studies are glycosidases, which act upon polyhydroxylated substrates. Interactions with the hydroxyls must be important and can be probed, individually, by measuring kinetic parameters for a series of substrates that have been, individually, deoxygenated at each position. Of particular interest in this regard are interactions with the hydroxyl group adjacent to the anomeric carbon (the 2-hydroxyl), which appear to be universally strong in retaining β-glycosidases that act upon glycosides with equatorial 2-hydroxyls (e.g., β-glucosidases, β-galactosidases, cellulases). The 2-hydroxyl typically contributes 5−10 kcal mol^{-1} to catalysis in these enzymes, whereas the other sugar ring hydroxyls contribute 1−2 kcal mol^{-1} (*1*−*4*). Furthermore, close interaction (∼2.5 Å) of the nucleophile carboxyl oxygen and the 2-hydroxyl (or fluorine) has been observed by crystallographic analysis of trapped covalent intermediates (*5*, *6*). From these observations it is believed that a strong hydrogen bond forms between the 2-hydroxyl and the nonreacting oxygen of the nucleophilic carboxylate in the oxocarbenium ion transition state (Figure 1a). The close approach of the 2-hydroxyl and nucleophile would be encouraged in such a transition state as the pyranose ring adopts a flattened half-chair ($^4H_3$) conformation and the nucleophile begins to attack anomeric carbon. Likewise, the development of positive charge at the anomeric carbon can be expected to transiently acidify the 2-hydroxyl ($pK_a \sim 12$), making it a better hydrogen bond donor to the nucleophile ($pK_a \sim 4-5$). The importance of the 2-hydroxyl is underscored by the potency of novel transition state analogues that exploit this interaction (*7*, *8*).

† This work was supported by the Protein Engineering Network of Centres of Excellence of Canada (PENCE) and the Natural Sciences and Engineering Research Council of Canada (NSERC). D.L.Z. thanks the Izaak Walton Killam Foundation and NSERC for fellowships.

* Corresponding author. E-mail: withers@chem.ubc.ca.

‡ PENCE and Department of Chemistry, University of British Columbia.

§ PENCE and Department of Microbiology, University of British Columbia.

10.1021/bi034329j CCC: $25.00
Published on Web 05/20/2003

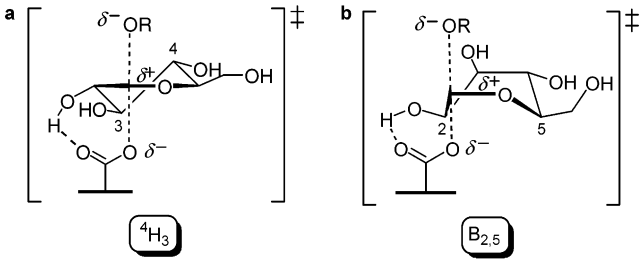

FIGURE 1: Comparison of pyranoside ring conformations and interaction of the catalytic nucleophile with the substrate 2-hydroxyl in a hypothetical β-glucosidase transition state (a) and β-mannosidase transition state (b).

It would appear that the opposite stereochemical configuration at C-2 in a β-mannoside substrate would exclude β-mannosidases and β-mannanases from utilizing the catalytic nucleophile in this fashion. Nevertheless, a recent crystallographic description of a β-mannanase reaction coordinate suggests that a unique $B_{2,5}$ mannoside ring conformation may in fact allow close approach of the mannose 2-hydroxyl to the nucleophile (Figure 1b) (*9*). These observations have prompted us to explore the reaction mechanism of a family 2 β-mannosidase from *Cellulomonas fimi* (Man2A)[1] (*10*). The active site nucleophile has previously been identified as E519 by labeling with a mechanism-based inactivator (*11*), and sequence homology with other family 2 glycosidases suggests that E429 is the general acid−base catalyst (*10*). In this study the reaction mechanism of Man2A has been characterized by Brønsted correlations, kinetic isotope effects, site-directed mutagenesis, and chemical rescue with fluoride and azide. The contribution of the 2-hydroxyl to catalysis has also been examined.

MATERIALS AND METHODS

General. The synthesis and characterization of the aryl mannoside substrates used in this study will be published elsewhere. Syntheses of other substrates are provided in the Supplementary Information. The cloning, expression, and purification of *C. fimi* β-mannosidase have been described previously (*10*).

Steady-State Kinetic Analyses of Man2A and Man2AE429A. Steady-state kinetic analyses were performed on Unicam UV-4 or Unicam 8700 UV−vis spectrometers equipped with thermoequilibrated cell blocks. All reactions were performed at 25 °C, pH 7, in acrylic cuvettes unless otherwise noted. A typical reaction cuvette contained substrate, 50 mM sodium phosphate (pH 7), and 1 mg/mL BSA in a total volume of 750 μL. After the cuvette was preequilibrated at 25 °C, a small aliquot of appropriately diluted Man2A (5−10 μL in 1 mg/mL BSA) was added and mixed briefly. Release of the phenol was monitored continuously at the appropriate wavelength. Initial rates (V_i) were determined from linear fits of these plots in regions corresponding to 5−15% consumption of the substrate. Substrate concentrations were varied typically from one-fifth to five times the final K_m value, whenever possible, for Michaelian kinetics. Higher substrate concentrations were assayed when substrate inhibition was observed. Steady-state kinetic parameters were derived by fits of the data to the Michaelis−Menten equation or the substrate inhibition equation (eq 1) using GraFit (*12*).

$$\frac{V_i}{E_t} = \frac{k_{cat}[S]}{K_m + [S] + [S]^2/K_i} \quad (1)$$

The wavelengths and extinction coefficients used for assays of aryl β-mannosides and calculation of k_{cat} are the same as those reported previously (*13*). The substrate 4-methylumbelliferyl β-mannoside was assayed at 365 nm ($\Delta\epsilon = 5136\ M^{-1}\cdot cm^{-1}$) (*14*).

Assays with 4-chlorophenyl and phenyl β-mannoside were performed in quartz cuvettes (500 μL total volume). Stock solutions of 2,4DNPMan were prepared immediately before use in an acidic buffer (pH 5−6), and concentrated aliquots (5−50 μL) of the substrate were used to initiate reaction with Man2A in pH 7 buffer. In neutral solutions, 2,4DNP-Man slowly rearranges to a new species, presumably through a migration of the 2,4-dinitrophenyl group to the 2-hydroxyl. This migration is very rapid above pH 7. The rearranged species can be observed by TLC (UV and acid charring): R_f for 2,4DNPMan (7:2:1 EtOAc/MeOH/H_2O) = 0.65; R_f for the migration product = 0.74.

Concentrations of Man2A and Man2A E429A stock solutions were determined by absorbance at 280 nm using the extinction coefficient 210000 $M^{-1}\cdot cm^{-1}$ (calculated from the amino acid sequence) (*15*).

pH−Rate Studies. The pH dependence of k_{cat}/K_m for wild-type Man2A was determined by generating first-order rate curves at low substrate concentrations ([S] $\ll K_m$). Cuvettes were charged with the appropriate buffer, 1 mg/mL BSA, and a concentration of substrate that was one-tenth or less of the corresponding K_m value (9.3 μM 4NPMan, 205 μM PhMan). After equilibration at 25 °C an aliquot of Man2A (10 μL) was added to afford a final concentration of enzyme sufficient to generate a first-order rate of phenol release within 10−20 min (0.12 μM Man2A for 4NPMan, 2.1 μM Man2A for PhMan). Phenol release was monitored continuously on a Unicam UV-4 spectrometer (λ = 400 nm for 4NPMan, 280 nm for PhMan) until a limiting absorbance was reached. The first-order rate curves generated at each pH value were fit using GraFit to the first-order rate equation (eq 2) to determine the rate constant k, which corresponds

$$A_t = A_\infty(1 - e^{-kt}) + \text{offset} \quad (2)$$

to V_{max}/K_m. The following buffers (50 mM) were used for the following pH ranges: citric acid, pH 6−6.8; sodium phosphate, pH 6.8−8.4. Man2A retained at least 90% activity in these buffers at each pH over a period of 30 min. Rates were obtained at overlapping buffer pH values, and buffer concentrations were varied to reveal buffer effects, none of which were observed. The k_{cat}/K_m values determined at each pH were fit with a function describing a single ionization

[1] Abbreviations: Man2A, *Cellulomonas fimi* β-mannosidase; BSA, bovine serum albumin; PE, petroleum ether (30−60 °C); EtOAc, ethyl acetate; MES, 2-(*N*-morpholino)ethanesulfonic acid; AMPSO, 3-[(1,1-dimethyl-2-hydroxyethyl)amino]-2-hydroxypropanesulfonic acid; α-D-KIE, α deuterium kinetic isotope effect; α-$D^{(V)}$, α deuterium kinetic isotope effect on V_{max}; 2,4DNPMan, 2,4-dinitrophenyl β-mannoside; 2,5DNPMan, 2,5-dinitrophenyl β-mannoside; 4NPMan, 4-nitrophenyl β-mannoside; 4NPC, 4-nitrophenyl β-cellobioside; PhMan, phenyl β-mannoside; α-manF, α-mannosyl fluoride.

using GraFit (eq 3).

$$k_{cat}/K_m = \frac{\text{limit}_1 + \text{limit}_2 \times 10^{pH-pK_a}}{10^{pH-pK_a} + 1} \quad (3)$$

In the case of Man2A E429A the pH dependence of k_{cat}/K_m for the reaction with 2,5DNPMan could not be determined owing to the very low K_m value (<1 μM) with this substrate. Therefore, k_{cat} was determined from initial rates at various pH values using a single saturating concentration of 2,5DNPMan (2 mM). An extinction coefficient of 4288 $M^{-1}\cdot cm^{-1}$ ($\lambda = 440$ nm) for 2,5-dinitrophenol ($pK_a^{lg} = 5.15$) was used for pH values between 6 and 9, and a value of 2290 $M^{-1}\cdot cm^{-1}$ for pH 5.5, to determine k_{cat}. The following buffers (50 mM) were used: MES, pH 5.5−6.9; sodium phosphate, pH 6.75−8.2; AMPSO, pH 8.85−9.1. A dramatic buffer effect was observed for 50 mM citric acid between pH 5.5 and pH 7 that was dependent on the concentration of citrate. The k_{cat} values at each pH were fit with a function describing a bell-shaped pH profile (eq 4) using GraFit.

$$k_{cat} = \frac{\text{limit} \times 10^{pH-pK_{a1}}}{10^{2pH-pK_{a1}-pK_{a2}} + 10^{pH-pK_{a1}} + 1} \quad (4)$$

Azide and Fluoride Rescue of Man2A E429A. A stock solution of sodium azide (0.5 M) in 50 mM sodium phosphate, pH 7, was prepared within a day of use and stored at 0−4 °C. Initially, Man2A E429A was assayed under standard conditions (1 mg/mL BSA, pH 7, 25 °C) with a single saturating concentration of 2,5DNPMan (2 mM) while varying the concentration of azide (1−200 mM). Apparent k_{cat} and K_m values were obtained by fixing azide at 100 mM and varying the concentration of 2,5DNPMan from one-fifth to five times the final K_m value. Spontaneous hydrolysis of 2,5DNPMan was negligible at all concentrations.

The fluorination of 2,5DNPMan with Man2A E429A was performed with 1 M KF, 1 mg/mL BSA, and 100 mM sodium phosphate, pH 7, at 25 °C. Reactions with NaCl, KCl, or NaBr were performed under the same conditions. The release of 2,5-dinitrophenol was monitored spectrophotometrically at 440 nm ($\Delta\epsilon = 4288$ $M^{-1}\cdot cm^{-1}$).

Azide and Fluoride Rescue of Man2A Nucleophile Mutants. Solutions of 2,4DNPMan and azide, buffered at pH 6, were prepared immediately prior to use. The pH dependence of azide rescue with Man2A E519S was initially examined (data not shown). A marked increase in rate was observed with decreasing pH, which continued beyond the range of stability of the mutant (pH 5). For this reason all chemical rescue studies were performed at pH 6 (1 M azide, 100 mM citrate, 1 mg/mL BSA, pH 6, 25 °C). The release of 2,4-dinitrophenol was monitored spectrophotometrically (λ 400 nm, $\Delta\epsilon = 10900$ $M^{-1}\cdot cm^{-1}$) and corrected for spontaneous hydrolysis of the substrate, which was generally negligible at the concentrations of substrate used. Final enzyme concentrations of 184 nM E519A and 71 nM E519S were used. Man2A E519S displayed transglycosylation behavior at high substrate concentrations; therefore, kinetic parameters were derived from a fit of the data at low substrate concentrations to the Michaelis−Menten equation using GraFit. Man2A E519A displayed substrate inhibition; thus the whole data set was fit to the substrate inhibition equation.

Fluorination reactions with Man2A nucleophile mutants were performed in 2 M KF, 1 mg/mL BSA, and 100 mM citrate, pH 6, at 25 °C. Because concentrated solutions of fluoride destroy pH electrodes, the pH value was determined with precision litmus paper (Merck). Data points prior to the onset of transglycosylation in plots of reaction velocity versus substrate concentration were fit with the Michaelis−Menten equation to derive k_{cat} and K_m values.

Synthesis of β-D-Mannopyranosyl Azide with Man2A E429A. 2,5DNPMan (10.5 mg) was dissolved in 150 mM ammonium bicarbonate (1 mL, pH 7.9) containing 64 mM sodium azide. Man2A was added to afford a final enzyme concentration of 3.9 μM and the reaction incubated at room temperature overnight. TLC analysis indicated reasonably clean conversion to a new product that was not UV active. The reaction mixture was concentrated in vacuo and purified by silica gel chromatography (17:2:1 to 7:2:1 EtOAc/MeOH/H_2O). Evaporation of the solvent afforded β-mannosyl azide as a white film.

Kinetic Isotope Effects with Man2A E429A. α-DKIE's were determined on k_{cat} for Man2A E429A using virtually identical and saturating concentrations of 2,5-DNPMan and 2,5-DNP β-[1-^{2}H]mannoside (2 mM). A stock solution containing 1.1 μM Man2A E429A, 1 mg/mL BSA, and 50 mM sodium phosphate, pH 7, was prepared. Aliquots (700 μL) of the stock solution were then measured into quartz cuvettes and individually weighed on an analytical balance. After preequilibration at 25 °C, reaction was initiated by the addition of substrate (50 μL of a 30 mM stock solution), also preequilibrated at 25 °C. The reaction was monitored spectrophotometrically, as described above. A total of six to eight measurements were made with each substrate, alternating between each to eliminate bias. All initial rates (protio and deuterio) were corrected according to the corresponding masses of the reaction solutions. Measurements with 100 mM sodium azide or 100 mM NaCl were performed in the same fashion, with the corresponding stock solutions containing these salts.

Enzymatic Synthesis of α-D-Mannopyranosyl Fluoride. Man2A E519S or E519A (1 mg/mL) was reacted with 2,4DNPMan (19 mM) and 2 M KF in 100 mM citrate, pH 6, in a total volume of 1.5 mL. After 6 h at room temperature the reaction mixture was diluted 3-fold with acetonitrile, applied to a plug of silica gel, and eluted with 1 column volume of acetonitrile. The desalted sample was then dried in vacuo and analyzed by TLC (7:2:1 EtOAc/MeOH/H_2O). The remaining reaction mixture was subsequently acetylated with 3:2 pyridine/acetic anhydride and purified by silica gel chromatography (3:1 PE/EtOAc) to yield α-mannopyranosyl fluoride per-*O*-acetate as a clear gum. An analogous reaction with wild-type Man2A (0.12 mg/mL) monitored by ^{19}F NMR (282 MHz, 300 K) did not show any signals corresponding to the formation of α- or β-mannosyl fluoride.

β-D-Mannopyranosyl Fluoride. Man2A E429A (0.38 mg/mL, 4 μM) was reacted with 2,5DNPMan (23 mM) in 1 M KF, 100 mM sodium phosphate, and 10% D_2O, pH 7 (total reaction volume of 0.6 mL). The reaction was monitored by ^{19}F NMR (282 MHz) for 20−30 min at 300 K.

RESULTS

Substrate Reactivity and Brønsted Analysis of Man2A. The steady-state rate behavior of Man2A displayed pronounced

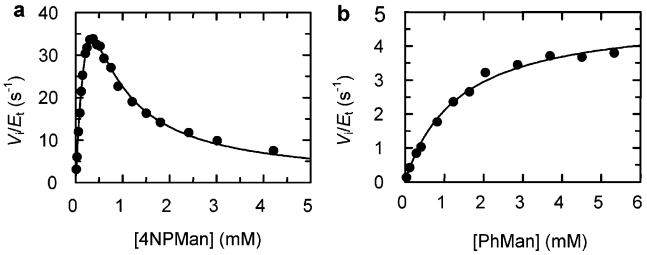

FIGURE 2: Plots of reaction velocity (V_i/E_t) versus substrate concentration for Man2A-catalyzed hydrolyses of 4NPMan and PhMan.

Table 1: Kinetic Parameters for the Reaction of Man2A with Substituted Aryl β-Mannosides (pH 7, 25 °C) Determined with Equation 1[a]

aglycon	pK_a^{lg}	k_{cat} (s^{-1})	K_m (mM)	K_i (mM)	k_{cat}/K_m (s^{-1}·mM^{-1})
2,4-dinitrophenyl	3.96	119 (6)	0.27 (0.02)	1.02 (0.09)	440
2,5-dinitrophenyl	5.15	150 (20)	0.42 (0.08)	0.24 (0.04)	364
4-chloro-2-nitrophenyl	6.45	230 (50)	0.8 (0.2)	0.19 (0.05)	290
4-nitrophenyl	7.18	179 (9)	0.78 (0.05)	0.16 (0.01)	230
methylumbelliferyl	7.6	61 (4)	0.19 (0.02)	0.47 (0.05)	320
3-nitrophenyl	8.39	33 (5)	0.5 (0.1)	0.15 (0.04)	66
4-chlorophenyl	9.4	7 (1)	0.36 (0.08)	1.3 (0.3)	19
phenyl	9.99	7.9 (0.4)	2.7 (0.2)	8.8 (0.8)	3

[a] Values in parentheses correspond to error limits of the curve fit.

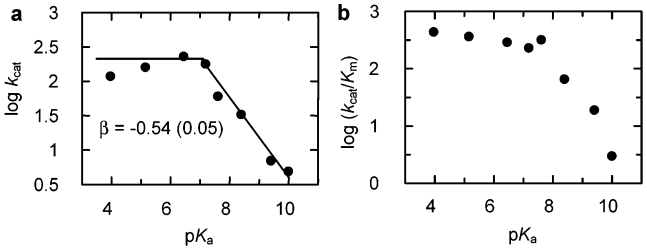

FIGURE 3: Dependence of log k_{cat} (a) and log(k_{cat}/K_m) (b) on pK_a^{lg} for wild-type Man2A-catalyzed hydrolyses of aryl β-mannosides.

substrate inhibition with virtually all aryl β-mannosides (Figure 2a). An exception was observed for the least reactive of the series, PhMan ($pK_a^{lg} = 9.99$), which followed normal saturation behavior within the same concentration range as the other substrates, although at higher concentrations (>6 mM) modest inhibition was observed (Figure 2b). Table 1 lists the kinetic parameters determined for the reaction of Man2A with aryl β-mannosides using eq 1.

A Brønsted plot of log k_{cat} versus the pK_a of the leaving group reveals an apparent downward break in the correlation occurring at $pK_a \sim 7$ (Figure 3a). The slope of the leaving group-dependent section of the Brønsted plot yields a β_{lg} value of -0.54 ± 0.05. The corresponding Brønsted plot for k_{cat}/K_m also shows a nonlinear, downward breaking correlation (Figure 3b).

A complementary experiment to the Brønsted analysis above is to examine the effect of an external neutral nucleophile on the steady-state rate (*16*). The rate of reaction of Man2A with the reactive substrate 2,5DNPMan increased linearly with the addition of ethylene glycol (Figure 4a). In contrast, ethylene glycol had essentially no effect on the rate of reaction with PhMan (Figure 4b). The slope of the plot for the 2,5DNPMan data yields an apparent second-order rate constant $k_{nuc}^{app} = 0.0203$ (± 0.0005) s^{-1} mM^{-1} for the reaction with ethylene glycol, whereas $k_{nuc}^{app} = 0.0009$ (± 0.0003) s^{-1} mM^{-1} for the reaction with PhMan. A similar apparent increase in reaction rate has been observed for the analogous reaction with *Escherichia coli* (*lacZ*) β-galactosidase (*17*, *18*).

pH−Rate Dependence of Man2A. The pH dependence of k_{cat}/K_m for the reaction of Man2A with two different substrates was examined (Figure 5). In each case k_{cat}/K_m shows an apparent dependence on a single ionization event. Essentially identical pK_a values were observed with 4NPMan ($pK_a = 7.6 \pm 0.1$) and PhMan ($pK_a = 7.7 \pm 0.1$). The pH behavior of Man2A below pH 5 could not be examined due to instability of the enzyme in this pH range.

Identification of the General Acid−Base Catalyst in Man2A and Chemical Rescue. Alignment of the sequence of Man2A with those of other family 2 glycosidases, including two for which three-dimensional structures are available, indicated that E429 was most likely the acid−base catalyst (Figure 6). The corresponding mutant E429A was found to hydrolyze only the most reactive of substrates (2,4DNPMan and 2,5DNPMan). Kinetic parameters of $k_{cat} = 12$ min^{-1} and $K_m < 1$ μM were determined for the reaction with 2,5DNPMan. Saturating kinetic behavior was observed for the reaction of 2,5DNPMan with Man2A E429A, although at high substrate concentrations (3−4 mM) very weak substrate inhibition was perceptible (data not shown). This contrasts sharply with the severe substrate inhibition observed with the wild-type enzyme (Figure 2a).

The dependence of k_{cat} on pH for the reaction of 2,5DNPMan with Man2A E429A was described by two ionizations

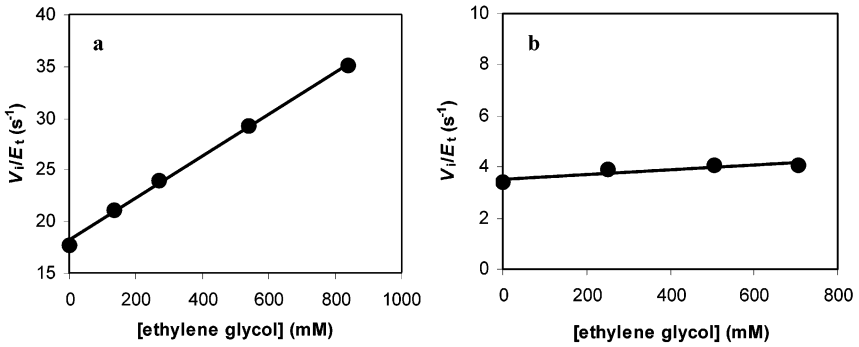

FIGURE 4: Dependence of the reaction rate of Man2A wt with saturating substrate and added ethylene glycol: (a) 2,5-dinitrophenyl β-mannoside (3.8 mM); (b) phenyl β-mannoside (10.6 mM). Lines are linear regressions of the data.

Table 2: Kinetic Parameters for Glycosylation Reactions Catalyzed by Man2A Nucleophile Mutants

	k_{cat} (min^{-1})	K_m (mM)	k_{cat}/K_m (min^{-1}·mM^{-1})	behavior at high [S]
Man2A wt[a]	27000	0.6	45000	substrate inhibition, $K_i = 0.31 \pm 0.06$ mM
+2 M KF[a]	7900	0.22	36000	substrate inhibition
Man2A E519A [a]	<0.008			
+1 M azide[a]	174	0.193	901	substrate inhibition, $K_i = 42 \pm 4$ mM
+2 M KF[a]	20.7	0.131	158	transglycosylation
+α-manF (20 mM 4NPC)[b]	0.33	0.57	0.56	saturation
+4NPC (50 mM α-manF)[b]			0.013	linear
Man2A E519S[a]	0.0015			
+1 M azide[a]	25.2	0.044	573	transglycosylation
+2 M KF[a]	14.0	0.036	389	transglycosylation
+α-manF (29 mM 4NPC)[b]	12	0.70	17	saturation
+4NPC (50 mM α-manF)[b]			0.35	linear
Man2A E429A[c]	12	<0.001		saturation
+0.1 M azide[c]	221	0.025	8840	saturation
+1 M KF[c]	87	0.0077	11300	saturation

[a] Reaction with 2,4DNPMan (pH 6, 25 °C). Fluoride data from ref *20*. [b] Mannosynthase-catalyzed reaction (pH 6, 25 °C) reported in ref *21*. [c] Reaction with 2,5DNPMan (pH 7, 25 °C) (*20*).

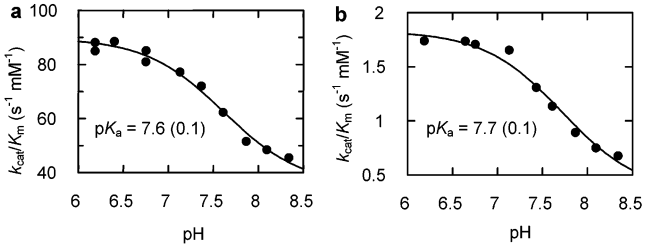

FIGURE 5: Dependence of k_{cat}/K_m on pH for the reaction of 4NPMan (a) and PhMan (b) with Man2A (25 °C).

	*⇓	
Man2A (AF126472)	HASLVLWNGGNEN	430
Human β-mannosidase (U60337)	HPSIIIWSGNNEN	457
E. coli (*lacZ*) β-galactosidase (J01636)	HPSVIIWSLGNES	462
Human β-glucuronidase (M15182)	HPAVVMWSVANEP	452

FIGURE 6: Alignment of a section of the amino acid sequence of Man2A with those of selected family 2 glycosidases. Conserved residues are shown in bold. The acid−base catalyst is indicated with an arrow. The Asn that interacts with the 2-hydroxyl is indicated with an asterisk. GenBank codes are in parentheses.

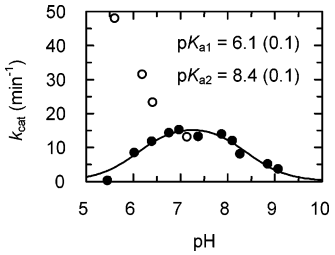

FIGURE 7: Dependence of k_{cat} on pH for the reaction of 2,5DNPMan with Man2A E429A (25 °C). Open circles represent rates obtained in citric acid buffer. The curve is a fit of the data (filled circles) by a double ionization function. The calculated pK_a values are indicated.

corresponding to pK_a's of 6.1 and 8.4 (Figure 7). Intriguingly, citric acid activates the mutant in a pH-dependent manner (Figure 7, open circles), an effect that was not observed with the wild-type enzyme.

A major enhancement of activity is observed for the reaction of 2,5DNPMan with Man2A E429A in the presence of azide. Saturating kinetic behavior is observed for k_{cat} as a function of azide concentration with an apparent K_m value of 0.56 mM (data not shown). The reaction of Man2A E429A with 2,5DNPMan in the presence of "saturating" azide (100 mM) produced an ~18-fold increase in k_{cat} and the substrate K_m also increased to 25 μM (Table 2). The azide rescue reaction was performed on a preparative scale to yield β-D-mannopyranosyl azide as the major product: R_f (7:2:1 EtOAc/MeOH/H_2O) = 0.61; ^{1}H NMR (200 MHz, CD_3OD) δ 4.58 (d, 1 H, J = 1.0 Hz, H-1), 3.91 (dd, 1 H, J = 2.3, 12.0 Hz, H-6a), 3.86 (dd, 1 H, J = 1.0, 3.1 Hz, H-2), 3.73 (dd, J = 6.0, 11.9 Hz, H-6b), 3.58 (dd, 1 H, J = 9.3, 9.3 Hz, H-4), 3.45 (dd, 1 H, J = 3.0, 9.3 Hz, H-3), 3.32 (ddd, 1 H, J = 2.3, 6.0, 9.3 Hz, H-5).

The turnover of Man2A E429A was also facilitated by fluoride, reaching a maximum rate at 1 M KF (data not shown). An approximately 7-fold increase in k_{cat} was observed with 1 M fluoride, and the K_m increased to ~8 μM (Table 2), whereas lesser but notable enhancements were observed with chloride (55%) and bromide (~10%). When the reaction was monitored directly by ^{19}F NMR spectroscopy (Figure 8a), a resonance corresponding to a low steady-state concentration of β-mannosyl fluoride was observed (δ −146.7 ppm, apparent doublet, J = 49 Hz, referenced to $CFCl_3$). This resonance matched the ^{19}F NMR spectrum of an authentic sample of β-D-mannosyl fluoride (Figure 8b) (*19*), which is clearly distinct from the spectrum of α-D-mannosyl fluoride (Figure 8c, δ −139.0 ppm, apparent doublet, J = 49 Hz, referenced to $CFCl_3$).

Kinetic Isotope Effects. The α-DKIE value on k_{cat} (α-D$^{(V)}$) was measured with the mutant E429A using the substrate 2,5-dinitrophenyl β-[1-^{2}H]mannoside and the protio analogue under saturating conditions (2 mM). A significant α-D$^{(V)}$ value of 1.12 ± 0.01 was observed (average of seven measurements). Doubling the concentration of deuterio and protio substrates afforded the same α-D$^{(V)}$ value, indicating that this effect is not the result of a contaminant in either substrate. Surprisingly, α-D$^{(V)}$ increased substantially to 1.166 ± 0.009 (six determinations) in the presence of 100 mM azide. This is an effect that is specific to the nucleophilicity of azide and not a nonspecific salt effect, because the same measurement in 100 mM NaCl afforded an α-D$^{(V)}$ value of 1.111 ± 0.007 (three determinations).

Azide and Fluoride Rescue of Man2A E519A and E519S. As observed previously for nucleophile mutants of retaining glycosidases, substantial glycosidic bond cleaving activity

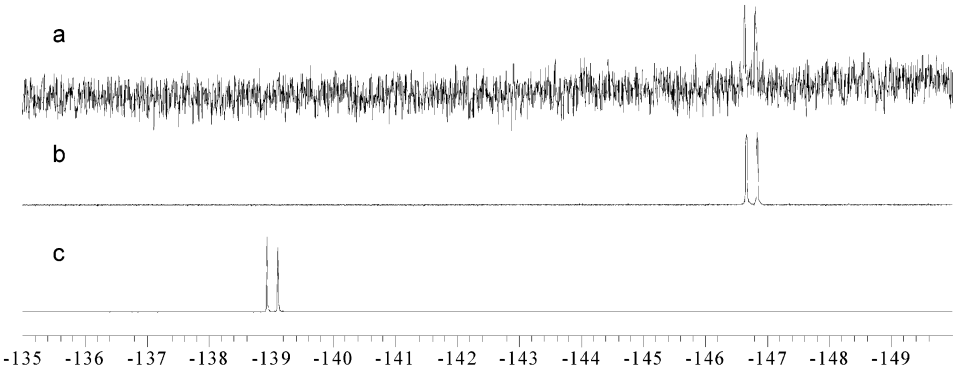

FIGURE 8: (a) ^{19}F NMR spectrum (282 MHz, referenced to $CFCl_3$) of the reaction of Man2A E429A with 2,5DNPMan in the presence of 1 M KF (pH 7, 300 K, 30 min). (b) Spectrum of β-D-mannosyl fluoride. (c) Spectrum of α-D-mannosyl fluoride.

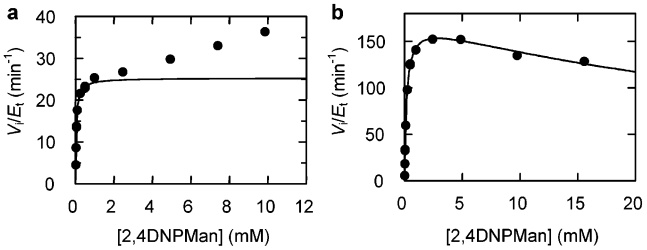

FIGURE 9: Reaction rate versus 2,4DNPMan concentration for the reaction with Man2A E519S (a) and E519A (b) in the presence of azide (1 M NaN_3, pH 6, 25 °C). The curves in (a) and (b) are fits of the data to the Michaelis−Menten and substrate inhibition equations, respectively.

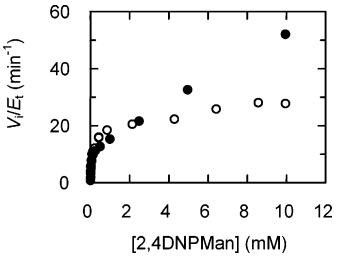

FIGURE 10: Plots of reaction velocity versus substrate concentration for the reaction of Man2A E519S (closed circles) and E519A (open circles) with 2,4DNPMan and fluoride (2 M KF, pH 6, 25 °C).

could be restored to Man2A nucleophile mutants with azide (Table 2). Virtually no activity could be detected with Man2A E519A or E519S in the absence of azide, even with the reactive substrate 2,4DNPMan. The addition of azide (1 M NaN_3, pH 6, 25 °C), however, increased k_{cat} values 17000−22000-fold. Transglycosylation behavior was observed at high substrate concentrations with the E519S mutant (Figure 9a), whereas substrate inhibition was observed with E519A (Figure 9b). As reported previously (*20*, *21*), fluoride also serves as a nucleophile with these mutants (Table 2), enhancing activity 2600−9000-fold (2 M fluoride, pH 6, 25 °C). Transglycosylation behavior was observed with both mutants at high substrate concentrations (Figure 10). This is consistent with the in situ formation of α-mannosyl fluoride that is subsequently used to glycosylate a second equivalent of substrate. Indeed, TLC analysis of the reaction mixture indicated the formation of α-D-mannosyl fluoride as the major product [R_f (7:2:1 EtOAc/MeOH/H_2O) = 0.58]. ^1H and ^{19}F NMR spectra of the isolated, per-O-acetylated product agreed with those of an authentic sample of α-D-mannopyranosyl fluoride per-*O*-acetate: R_f (2:1 PE/EtOAc) = 0.53; ^1H NMR (200 MHz, $CDCl_3$) δ 5.55 (dd, 1 H, J = 48.3, 1.7 Hz, H-1), 5.40−5.30 (m, 3 H, H-2,3,4), 4.29 (dd, 1 H, J = 12.7, 5.4 Hz, H-6a), 4.14 (m, 2 H, H-5, H-6b); ^{19}F NMR (188 MHz, $CDCl_3$, referenced to CF_3CO_2H) δ −62.5 (d, J = 49.2 Hz).

Evaluating the Role of the 2-Hydroxyl in Catalysis. A linear relationship of reaction velocity versus substrate concentration was observed for the reaction of Man2A with the 2-deoxy analogue 4-nitrophenyl 2-deoxy-β-D-*arabino*-hexopyranoside. While the lack of saturation behavior precluded determination of individual values of k_{cat} and K_m, it did allow a value of k_{cat}/K_m to be determined. A comparison of k_{cat}/K_m values for 4NPMan (230 s^{-1} mM^{-1}) and 4-nitrophenyl 2-deoxy-β-D-*arabino*-hexopyranoside (0.039 s^{-1} mM^{-1}) indicates a 5900-fold reduction in this parameter as a result of the removal of the 2-hydroxyl or a $\Delta\Delta G^{\ddagger}$ value of 5.1 kcal mol^{-1}.

DISCUSSION

Substrate Inhibition and Brønsted Analysis of Man2A. The steady-state rate behavior of Man2A displayed substrate inhibition with all aryl β-mannosides except the least reactive of the series, PhMan (Figure 2). Substrate inhibition occurs when a second molecule of substrate binds to the Michaelis complex of the enzyme, resulting in a ternary complex that has reduced activity (Figure 11). This is not an unknown behavior for glycosidases (*14*, *22*, *23*), which frequently have long active site clefts to accommodate multiple monosaccharide units of a polysaccharide chain and, thus, have the potential to bind two substrate molecules simultaneously in an unproductive fashion. In the case of a retaining glycosidase a second type of ternary complex may arise from a substrate-inhibited covalent intermediate (Figure 11b). In order for this to occur at a kinetically significant level the covalent intermediate species must be sufficiently abundant to receive a second substrate molecule. The resulting ternary complex may be a true dead-end species (*22*) or possibly a transglycosylation complex in which the subsequent transglycosylation step (k_{trans}) is slower than the hydrolysis pathway (k_{hydro}) (*24*, *25*). This latter model is a possibility with Man2A because the wild-type enzyme does catalyze transglycosylation with the substrate 4NPMan (data not shown). This may explain why the least reactive substrate, PhMan, elicits weak substrate inhibition and possibly why the acid−base mutant E429A does not display substrate inhibition (see below). If the Michaelis and covalent intermediate enzyme species in Figure 11b are combined, as well

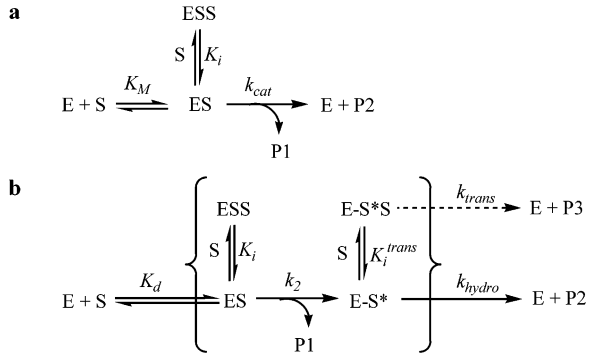

FIGURE 11: (a) Simplified kinetic scheme for substrate inhibition. (b) Proposed kinetic scheme for substrate inhibition of Man2A (E) during the hydrolysis of an aryl β-mannoside (S). ES = Michaelis complex; E−S* = covalent intermediate; ESS = substrate-inhibited Michaelis complex; E−S*S = substrate-inhibited covalent intermediate or transglycosylation complex; K_i and K_i^{trans} are inhibition (dissociation) constants for the second substrate molecule; P1 = phenol; P2 = mannose; P3 = disaccharide transglycosylation product.

as the corresponding inhibition pathways, the standard equation for substrate inhibition may be used (eq 1).

The Brønsted plot of log k_{cat} versus the pK_a of the leaving group (Figure 3a) displays a concave downward break that implies a change in rate-determining step. This plot is consistent with the double displacement mechanism of a retaining glycosidase and reports on the deglycosylation step with the reactive substrates (p$K_a^{lg} \leq 7$) and the glycosylation step with the less reactive substrates (p$K_a^{lg} > 7$). Support for this assertion comes from the ability to partition the covalent intermediate with an exogenous neutral nucleophile. Because the covalent intermediate will react faster with an acceptor more nucleophilic than water, an increase in rate can be expected for substrates for which deglycosylation is rate limiting. Accordingly, the rate of reaction of Man2A with 2,5DNPMan is increased by added ethylene glycol (Figure 4a) but not the rate of reaction with PhMan (Figure 4b). The β_{lg} value (-0.54 ± 0.05) obtained from the slope of the leaving group-dependent section of the Brønsted plot reflects a glycosylation transition state with approximately 50% negative charge development on the departing glycosidic oxygen. This value is notably less than values obtained for other retaining glycosidases, which typically have β_{lg} values of around -0.8 [$\beta_{lg} = -0.7$ for *Agrobacterium* sp. β-glucosidase (*13*) and $\beta_{lg} = -1$ for *C. fimi* endoglycanase (*26*)]. This suggests that significant differences exist in the glycosylation transition state for Man2A, such as in the degree of glycosidic bond cleavage and protonation of the glycosidic oxygen.

The corresponding Brønsted plot for k_{cat}/K_m also shows a nonlinear, downward breaking correlation (Figure 3b). A similar concave-down correlation has been observed for k_{cat}/K_m in a number of other cases, including *Agrobacterium* sp. β-glucosidase (*13*) and *Thermoanaerobacterium saccharolyticum* β-xylosidase (*27*). Since this parameter represents the second-order rate constant for the first irreversible step, which is generally agreed to be the glycosylation step, a break in the correlation is not expected unless substrate binding reaches diffusion control (10^8 s^{-1} M^{-1}). However, the k_{cat}/K_m values determined here are well below the diffusion limit. No satisfactory resolution to this anomalous kinetic behavior was arrived at previously for these other enzymes, though the most probable explanation is that the rate of release of the phenol drops substantially as the phenol pK_a drops, quite likely because of the formation of a strong hydrogen bond with the acid catalyst. In other words, the phenolate anion is "sticky", as had been proposed previously for a family 1 β-glucosidase (*28*). The kinetic consequence is that the glycosylation step is no longer functionally irreversible; thus the deglycosylation step becomes reflected in k_{cat}/K_m and, hence, a partial flattening of the plot.

pH−Rate Dependence of Man2A. The ionizations of the general acid−base catalyst and the nucleophile have been observed to dominate the pH−rate profiles of some other retaining glycosidases, such as *T. saccharolyticum* β-xylosidase (*29*), *Bacillus circulans* xylanase (*30*), and *C. fimi* exoglycanase (*31*, *32*). The k_{cat}/K_m value of Man2A varies with pH according to a single pK_a of 7.6 (Figure 5). Because k_{cat}/K_m reflects ionizations in the free enzyme and the free substrate, the ionization described by this pK_a value may originate from the acid−base catalyst of the free enzyme. At the pH optimum of this enzyme (6.5−7.0) a pK_a of 7.6 would set the required ionization state of the acid−base residue to perform acid catalysis in the glycosylation step, though caution is necessary in the interpretation of these data, as k_{cat}/K_m does not approach zero at high pH with either substrate (*30*). An ionization with a low pK_a (<5), as might be expected from the nucleophile, could not be observed with Man2A due to the instability of the enzyme below pH 5.5.

Identification of the General Acid−Base Catalyst in Man2A. An effective approach toward the identification of the general acid−base catalyst of a retaining glycosidase involves deletion of the predicted residue by site-directed mutagenesis followed by assessment of the resulting mutant by kinetic analysis and chemical rescue (*33*). Alignment of the amino acid sequence of Man2A with those of other family 2 glycosidases indicated that E429 was strictly conserved and matched the known acid−base catalyst in *E. coli* (*lacZ*) β-galactosidase (Figure 6) (*34*).

The corresponding mutant Man2A E429A was assayed with aryl β-mannoside substrates of varying reactivity. Only the substrates 2,4DNPMan and 2,5DNPMan were cleaved. These substrates possess good leaving groups (p$K_a^{lg} \leq 5.15$) that do not require acid catalysis in the glycosylation step. In contrast, no reaction was observed with 4-nitrophenyl or 3-nitrophenyl β-mannoside, consistent with an important role for E429 in the cleavage of substrates that need acid catalytic assistance (phenol p$K_a > 7$). Unlike the wild-type enzyme, saturating kinetic behavior was observed with Man2A E429A across a similar substrate concentration range. A plausible reason for this is that the wild-type substrate inhibition arises from a slow transglycosylation pathway (Figure 11b) that requires base-catalyzed deprotonation of an acceptor hydroxyl group.

Since base catalysis in the deglycosylation step is not possible for a mutant missing the acid−base catalyst, the deglycosylation step will also be very slow, and this will be true for all substrates, regardless of their aglycons. If the glycosylation step is accelerated sufficiently by use of a substrate with a reactive leaving group, then deglycosylation will be rate limiting for this substrate and the glycosyl-enzyme will accumulate. This was indeed evident from the low k_{cat} (12 min^{-1}) and K_m (<1 μM) values observed for

the reaction of Man2A E429A with 2,5DNPMan. Low K_m values arise in this case because the accumulation of the glycosyl-enzyme increases the denominator in the general expression for a K_m value:

$$K_m = [E][S]/\sum[ES]$$

where E is free enzyme, S is the substrate, and ES represents all enzyme−substrate species.

The pH dependence of k_{cat} for the reaction of the mutant with 2,5DNPMan follows a bell-shaped profile with pK_a's of 6.1 and 8.4 (Figure 7). As k_{cat} reports on the deglycosylation step for this mutant and because the mutant is supposedly missing the acid−base catalyst, these ionizations cannot be readily assigned. Direct ionization of the nucleophile is impossible during deglycosylation, and chemical rescue studies (described below) confirm that the acid−base catalyst is absent in the E429A mutant. Therefore, the ionizations must arise from other groups in the active site, such as those that interact with the nucleophile, or groups that assume the role of the base catalyst.

A characteristic of acid−base mutants of retaining glycosidases is the enhancement of catalytic activity observed with activated substrates when the mutant is provided a small anionic nucleophile such as azide (*33*). Unlike water, a small anion does not require general base catalysis to function as a nucleophile in the deglycosylation step and thus can react with the glycosyl-enzyme in mutants missing the acid−base catalyst, thereby increasing the turnover rate. Such enhancement of activity is observed for the reaction of 2,5DNPMan with Man2A E429A in the presence of azide. Saturation-like kinetic behavior is observed for k_{cat} as a function of azide concentration with an apparent K_m value of 0.56 mM. By analogy to rescue studies on *C. fimi* exoglycanase (*32*) and *E. coli* (*lacZ*) β-galactosidase acid−base mutants (*35*), the saturation observed with azide does not represent true binding of the anion in the active site. Instead, this reflects the change in rate-determining step as azide concentration is raised, such that eventually glycosylation becomes rate limiting. The kinetic parameters determined for E429A with 2,5DNPMan in the presence of saturating azide (100 mM) revealed an 18-fold increase in turnover number ($k_{cat} = 221 \pm 8$ min^{-1}) and a dramatic increase in the K_m value (25 ± 3 μM). The increase in both parameters is consistent with azide facilitating turnover of the covalent intermediate. This mechanism for azide rescue was confirmed by performing the reaction on a preparative scale and isolating β-D-mannopyranosyl azide as the major product.

Intriguingly, citric acid activates the mutant in a pH-dependent manner (Figure 7, open circles), an effect that was not observed with the wild-type enzyme. The activation by citric acid was also concentration-dependent, which suggests that this is a form of chemical rescue of the acid−base mutant. It is possible that citric acid could function as a general base catalyst or as a nucleophile in the deglycosylation step. The increase in rate as a function of decreasing pH at first appears to be inconsistent with both possibilities, since protonation of the carboxylates of citric acid would be expected to be deleterious to both roles. It is possible, however, that protonation of one of the other carboxyl groups of citric acid may be needed to allow it to bind in the Man2A E429A active site and perform chemical rescue. The pH dependence observed may therefore reflect this ionization. Such rescue behavior is quite common with mutants of the acid−base catalyst (vide infra) and has also been seen in a natural system wherein the family 1 plant myrosinases lack an acid−base catalyst but bind ascorbate to carry out this role (*36*).

We previously reported that the turnover of Man2A E429A was also dramatically enhanced with fluoride ($k_{cat} = 87$ min^{-1} and $K_m = 7.7$ μM, 1 M KF) (*20*). Substantially greater concentrations of fluoride than of azide were required to promote turnover, consistent with the lesser nucleophilicity of fluoride relative to azide. This enhancement is specific to the nucleophilicity of fluoride and is not merely a salt effect, because equivalent concentrations of NaCl, KCl, and KBr increased rates only modestly (~55% with 1 M chloride, ~10% increase with 1 M bromide). It is possible that chloride and perhaps bromide also function as weak nucleophiles with the E429A mutant, as such chemical rescue has been observed with nucleophile mutants of *Agrobacterium* sp. β-glucosidase (*20*). In this case the β-mannosyl fluoride product could not be directly isolated for it is also a good substrate for Man2A (*11*). Nevertheless, a ^{19}F NMR spectrum of the reaction mixture revealed a resonance that matched that of an authentic sample of β-mannosyl fluoride (Figure 8).

The energetic contribution of the acid−base catalyst to transition state stabilization can be calculated from the kinetic parameters measured with and without azide. Comparison of the k_{cat}/K_m value observed for Man2A E429A in the presence of 100 mM azide (8840 min^{-1} mM^{-1}) with that for the wild-type enzyme ($k_{cat}/K_m = 21840$ min^{-1} mM^{-1}) reveals a mere 2.5-fold rate difference. Because this parameter presumably reports on the glycosylation step in each case, the minimal reduction in rate as a result of eliminating acid catalysis is consistent with the good leaving group ability of 2,5-dinitrophenol, which requires minimal, if any, protonic assistance to depart. However, the deglycosylation rate, reflected by the corresponding k_{cat} values (12 min^{-1} for E429A in the absence of azide, 9000 min^{-1} for the wild type), is reduced 750-fold ($\Delta\Delta G^{\ddagger} = 3.9$ kcal mol^{-1}), reflecting the considerably greater need of base catalysis for the attack of water on the mannosyl-enzyme intermediate. This energetic cost is approximately half of that observed for the E461G acid−base mutant of *E. coli* (*lacZ*) β-galactosidase (Mg^{2+} form) using deglycosylation rate-limiting substrates (1300−1700-fold reduction in k_{cat}, $\Delta\Delta G^{\ddagger} = 4.2$−4.4 kcal mol^{-1}) (*35*, *37*).

Kinetic Isotope Effects on Reactions of E429A. Unlike the wild-type enzyme, the saturation kinetic behavior observed with the E429A mutant of Man2A allows facile measurement of the α-DKIE value on k_{cat}. The rate-limiting step for the E429A mutant with the reactive substrate 2,5-DNPMan is clearly deglycosylation. The significant value of $\alpha\text{-}D^{(V)} = 1.12 \pm 0.01$ observed for E429A indicates that this transition state has considerable oxocarbenium ion character. Accordingly, there must be only modest association of the substrate anomeric carbon with the incoming nucleophilic water and departing E519 carboxylate. Surprisingly, the $\alpha\text{-}D^{(V)}$ value increased substantially to 1.166 ± 0.009 with the strong nucleophile azide. This is initially surprising since a better nucleophile might have been expected to make the reaction more S_N2-like and thus have a lower kinetic isotope effect.

However, it must be remembered that the presence of azide changes the rate-determining step from deglycosylation to glycosylation for Man2A E429A. Therefore, the larger α-$D^{(V)}$ value measured with azide reports on the glycosylation transition state, which is itself not expected to involve azide. Having said this, a larger kinetic isotope effect for the glycosylation step than for the deglycosylation is also surprising since in other β-glycosidases the glycosylation transition state has *less* S_N1 character (i.e., has a smaller α-DKIE) than the deglycosylation transition state (*13*, *26*, *38*). The difference may have its root in the fact that the acid−base catalyst is missing in E429A, thereby affecting the amount of oxocarbenium ion character at each step. In the deglycosylation step, the absence of base catalysis will demand greater preassociation of the attacking water, thus producing the smaller α-$D^{(V)}$ value. In contrast, the presence of a very good leaving group such as 2,5-dinitrophenol allows negative charge development on the phenol oxygen in the absence of acid catalysis and thus promotes substantial bond cleavage to the anomeric carbon of the substrate. This would produce the larger α-$D^{(V)}$ value observed for the glycosylation step. Alternatively, it is possible that azide is present in the active site during the glycosylation step, thus introducing negative charge that will favor a more oxocarbenium ion-like transition state. Similar increases in α-DKIE values have also been observed for the reaction of *Botryodiplodia theobromae* β-glucosidase with glycerol when using substrates for which deglycosylation is rate-determining (*39*) and for the reaction of an acetal (bearing a good leaving group) with different nucleophiles (*40*).

Rescue of E519A and E519S with Fluoride and Azide. A second form of chemical rescue that is common with retaining glycosidases is replacement of the catalytic nucleophile carboxylate with small anions such as azide and formate (*33*). We have reported in previous publications that the virtually inactive nucleophile mutants E519S and E519A also regained impressive activity in the presence of fluoride (Table 2) (*20*, *21*). Intriguingly, the chemical rescue behavior of these mutants appears to correlate with their "mannosynthase" activity. As reported previously, Man2A E519S is a superior mannosynthase (*21*), with ~27-fold greater k_{cat}/K_m value than E519A for the reaction of α-mannosyl fluoride and 4-nitrophenyl β-cellobioside (Table 2), and this is tentatively attributed to a hydrogen-bonding interaction between the serine side chain of E519S and the departing fluoride of α-mannosyl fluoride (*41*). Likewise, a modestly greater k_{cat}/K_m value is observed for E519S (389 min^{-1} mM^{-1}) relative to E519A (158 min^{-1} mM^{-1}) for the reaction of fluoride with 2,4DNPMan (Table 2). Moreover, both nucleophile mutants exhibit nonsaturating reaction kinetics at high concentrations of 2,4DNPMan (Figure 10). Similar non-Michaelian plots have been observed in wild-type glycosidases that catalyze transglycosylation at high substrate concentrations (*13*, *27*). As with the kinetic parameters derived from the Michaelian regions of these curves, the relative slopes of the linear regions appear to correlate with the mannosynthase activity of the mutants. The k_{cat} value for Man2A E519S (12 min^{-1}) for the glycosylation of 4-nitrophenyl β-cellobioside with α-mannosyl fluoride is considerably greater than that for E519A (0.33 min^{-1}), and this is indeed reflected in the relative slopes of the transglycosylation regions of the plots in Figure 10.

As expected, considerable activity is also regained with azide (Table 2). However, unlike the case with fluoride, the E519S mutant has significantly lower azide rescue activity (k_{cat}/K_m = 573 min^{-1} mM^{-1}) relative to that of E519A (k_{cat}/K_m = 901 min^{-1} mM^{-1}). Although a hydrogen-bonding interaction between azide and serine may occur as proposed for fluoride, steric effects between azide and the serine side chain are most likely greater than for alanine. Steric effects are not likely to be crucial for the smaller fluoride anion with either mutant.

Evaluating the Role of the Substrate 2-Hydroxyl in Catalysis. The 2-deoxy substrate analogue 4-nitrophenyl 2-deoxy-β-D-*arabino*-hexopyranoside proved to be a slow substrate with wild-type Man2A, and unlike the parent substrate 4NPMan, saturating kinetic behavior was not observed, even up to high substrate concentrations. The absence of a measurable K_m value also implies that glycosylation is rate limiting with this substrate. A comparison of the k_{cat}/K_m values for 4NPMan (230 s^{-1} mM^{-1}) and 4-nitrophenyl 2-deoxy-β-D-*arabino*-hexopyranoside (0.039 s^{-1} mM^{-1}), which presumably report on the glycosylation step in both cases, indicates a 5900-fold reduction in this parameter as a result of the removal of the 2-hydroxyl ($\Delta\Delta G^{\ddagger}$ = 5.1 kcal mol^{-1}). This is likely a minimum estimate of the underlying effect, given the electron-withdrawing properties of the hydroxyl group, which tend to make glucosides inherently less reactive than their 2-deoxy counterparts.

The energetic contribution of the 2-hydroxyl in Man2A is comparable to that observed for the family 1 *Agrobacterium* sp. β-glucosidase (4.5 kcal mol^{-1}) (*2*) but is significantly less than the value obtained for the family 2 *E. coli* (*lacZ*) β-galactosidase (~8 kcal mol^{-1}) (*3*) and the family 10 *C. fimi* exoglycanase (~10 kcal mol^{-1}) (*1*). Nevertheless, the contribution of the substrate 2-hydroxyl to Man2A catalysis is substantial and indicates that key enzyme−substrate interactions are formed at this position in the transition state. Although it may at first appear geometrically impossible that a strong interaction between the enzyme nucleophile and the 2-hydroxyl could form in a β-mannosidase, a recent crystallographic analysis of reaction intermediates on a family 26 β-mannanase suggests otherwise (*9*). In this enzyme the β-mannoside substrate adopts novel $^1S_5$ and $^OS_2$ pyranoside ring conformations in the Michaelis and covalent intermediates, respectively, flanking what is likely a $B_{2,5}$ glycosylation transition state. These conformations maintain the 2-substituent in a pseudoequatorial position that appears to allow close approach to the nucleophile carbonyl oxygen (Figure 1b), as has been observed in glucosidases and cellulases (Figure 1a). The observation here of comparable interaction energies with those of other Clan GH-A glycosidases is consistent with a similar distorted conformation for Man2A. However, alternative substrate conformations and interactions with other residues in the Man2A active site cannot be excluded. An excellent candidate for a group that could take part in such interactions is N428, a fully conserved residue that is equivalent to N460 of *E. coli* (*lacZ*) β-galactosidase (Figure 6). This residue is located near the acid−base catalyst and has been observed crystallographically to form a hydrogen bond to the sugar 2-substituent in both the covalent intermediate and transition state analogue complexes (*34*). As discussed above, it may well be geometrically possible for N428 of Man2A to form a similar interaction with the

2-hydroxyl of a *manno*-configured substrate. A similarly located Asn residue interacts with the 2-hydroxyl of glucosides in family 1 glycosidases. Interestingly, one of the key differences between family 1 mannosidases and family 1 glucosidases is the fact that this residue is an Asp in the mannosidases, and mutation of this Asp residue to Asn switches the substrate specificity of family 1 mannosidases toward glucosides (*42*).

CONCLUSIONS

This study describes a detailed reactivity and mutational analysis of the retaining β-mannosidase from *C. fimi*, Man2A. A stunning feature of Man2A and its corresponding mutants is the range of chemistries that are catalyzed. Reactions ranging from hydrolysis of mannosides to the mannosylation of glycosides, azide, and fluoride are possible. In the latter case, "fluorination" of mannosides can be accomplished with both stereochemical outcomes. This behavior is not unique to Man2A as similar promiscuity has been observed with the retaining *Agrobacterium* sp. β-glucosidase (*20*). The rational engineering of fluorinase activity within a well-defined glycosidase may inform strategies to engineer such activity in completely different enzymes, which is particularly valuable when mechanistic information from natural fluorinases is lacking (*43*). The contribution of the β-mannoside 2-hydroxyl to Man2A catalysis ($\Delta\Delta G^{\ddagger} = 5.3$ kcal mol^{-1}) is comparable to that observed for glucosidases and cellulases that act on substrates with oppositely configured 2-hydroxyls. This is contrary to previous expectations (*44*) and suggests that the 2-hydroxyl is universally important to retaining β-glycosidase catalysis, regardless of the stereochemical configuration at C-2. This conclusion is reinforced by the fact that residues that appear to interact with the 2-hydroxyl are conserved in family 2. As suggested previously (*9*), this is consistent with the idea that interactions with the 2-hydroxyl as well as its orientation in the enzyme active site are conserved in glucosidase and mannosidase active sites simply by using different pyranoside conformations in each case, such as $B_{2,5}$ and $^4H_3$ (Figure 1). This implies that a part of the enzymatic recognition of mannosides versus glucosides may occur at hydroxyl groups that are farther from the reaction center, yet have very different orientations in space due to the conformations depicted in Figure 1.

SUPPORTING INFORMATION AVAILABLE

Details of the synthesis and characterization of 4-nitrophenyl 2-deoxy-β-D-*arabino*-hexopyranoside and β-mannosyl fluoride. This material is available free of charge via the Internet at http://pubs.acs.org.

REFERENCES

1. White, A., Tull, D., Johns, K., Gilkes, N. R., Withers, S. G., and Rose, D. R. (1996) *Nat. Struct. Biol. 3*, 149.
2. Namchuk, M. N., and Withers, S. G. (1995) *Biochemistry 34*, 16194.
3. McCarter, J., Adam, M., and Withers, S. G. (1992) *Biochem. J. 286*, 721.
4. Wolfenden, R., and Kati, W. M. (1991) *Acc. Chem. Res. 24*, 209.
5. Sidhu, G., Withers, S. G., Nguyen, N. T., McIntosh, L. P., Ziser, L., and Brayer, G. D. (1999) *Biochemistry 38*, 5346.
6. Notenboom, V., Birsan, C., Nitz, M., Rose, D. R., Warren, R. A. J., and Withers, S. G. (1998) *Nat. Struct. Biol. 5*, 812.
7. Williams, S. J., Notenboom, V., Wicki, J., Rose, D. R., and Withers, S. G. (2000) *J. Am. Chem. Soc. 122*, 4229.
8. Liu, H., Liang, X., Søhoel, H., Bülow, A., and Bols, M. (2001) *J. Am. Chem. Soc. 123*, 5116.
9. Ducros, V. M.-A., Zechel, D. L., Murshudov, G. N., Gilbert, H. J., Szabó, L., Stoll, D., Withers, S. G., and Davies, G. J. (2002) *Angew. Chem., Int. Ed. 41*, 2824.
10. Stoll, D., Stalbrand, H., and Warren, R. A. J. (1999) *Appl. Environ. Microbiol. 65*, 2598.
11. Stoll, D., He, S., Withers, S. G., and Warren, R. A. J. (2000) *Biochem. J. 351*, 833.
12. Leatherbarrow, R. J. (2001) GraFit 4.0, Erithacus Software, Ltd., London.
13. Kempton, J. B., and Withers, S. G. (1992) *Biochemistry 31*, 9961.
14. Malet, C., and Planas, A. (1997) *Biochemistry 36*, 13838.
15. Gill, S. C., and von Hippel, P. H. (1989) *Anal. Biochem. 182*, 319.
16. Fersht, A. (1999) *Structure and Mechanism in Protein Science: A guide to enzyme catalysis and protein folding*, W. H. Freeman, New York.
17. Richard, J. P., Westerfeld, J. G., Lin, S., and Beard, J. (1995) *Biochemistry 34*, 11713−24.
18. Viratelle, O. M., and Yon, J. M. (1973) *Eur. J. Biochem. 33*, 110.
19. Csuk, R., and Glänzer, B. I. (1988) *Adv. Carbohydr. Chem. Biochem. 46*, 73.
20. Zechel, D. L., Reid, S. P., Nashiru, O., Mayer, C., Stoll, D., Jakeman, D. L., Warren, R. A. J., and Withers, S. G. (2001) *J. Am. Chem. Soc. 123*, 4350.
21. Nashiru, O., Zechel, D. L., Stoll, D., Mohammadzadeh, T., Warren, R. A. J., and Withers, S. G. (2001) *Angew. Chem., Int. Ed. 40*, 417.
22. Brumer, H., III, Sims, P. F., and Sinnott, M. L. (1999) *Biochem. J. 339*, 43.
23. Zechel, D. L., He, S., Dupont, C., and Withers, S. G. (1998) *Biochem. J. 336*, 139.
24. Eneyskaya, E. V., Golubev, A. M., Kachurin, A. M., Savel'ev, A. N., and Neustroev, K. N. (1998) *Carbohydr. Res. 305*, 83.
25. Savel'ev, A. N., Ibatyllin, F. M., Eneyskaya, E. V., Kachurin, A. M., and Neustroev, K. N. (1996) *Carbohydr. Res. 296*, 261.
26. Tull, D., and Withers, S. G. (1994) *Biochemistry 33*, 6363.
27. Vocadlo, D. J., Wicki, J., Rupitz, K., and Withers, S. G. (2002) *Biochemistry 41*, 9727.
28. Dale, M. P., Ensley, H. E., Kern, K., Sastry, K. A. R., and Byers, L. D. (1985) *Biochemistry 24*, 3530.
29. Vocadlo, D. J., Wicki, J., Rupitz, K., and Withers, S. G. (2002) *Biochemistry 41*, 9736.
30. McIntosh, L. P., Hand, G., Johnson, P. E., Joshi, M. D., Korner, M., Plesniak, L. A., Ziser, L., Wakarchuk, W. W., and Withers, S. G. (1996) *Biochemistry 35*, 9958.
31. MacLeod, A. M., Tull, D., Rupitz, K., Warren, R. A. J., and Withers, S. G. (1996) *Biochemistry 35*, 13165.
32. MacLeod, A. M., Lindhorst, T., Withers, S. G., and Warren, R. A. (1994) *Biochemistry 33*, 6371.
33. Ly, H. D., and Withers, S. G. (1999) *Annu. Rev. Biochem. 68*, 487.
34. Juers, D. H., Heightman, T. D., Vasella, A., McCarter, J. D., Mackenzie, L., Withers, S. G., and Matthews, B. W. (2001) *Biochemistry 40*, 14781.
35. Richard, J. P., Huber, R. E., Heo, C., Amyes, T. L., and Lin, S. (1996) *Biochemistry 35*, 12387.
36. Burmeister, W. P., Cottaz, S., Rollin, P., Vasella, A., and Henrissat, B. (2000) *J. Biol. Chem. 275*, 39385.
37. Richard, J. P., Huber, R. E., Lin, S., Heo, C., and Amyes, T. L. (1996) *Biochemistry 35*, 12377.
38. Li, Y.-K., Chir, J., and Chen, F.-Y. (2001) *Biochem. J. 355*, 835.
39. Umezurike, G. M. (1988) *Biochem. J. 254*, 73.
40. Craze, G.-A., Kirby, A. J., and Osborne, R. (1978) *J. Chem. Soc., Perkin Trans. 2*, 357.
41. Mayer, C., Zechel, D. L., Reid, S. P., Warren, R. A. J., and Withers, S. G. (2000) *FEBS Lett. 466*, 40.
42. Kaper, T., van Heusden, H. H., van Loo, B., Vasella, A., van der Oost, J., and de Vos, W. M. (2002) *Biochemistry 41*, 4147.
43. O'Hagan, D., Schaffrath, C., Cobb, S. L., Hamilton, J. T., and Murphy, C. D. (2002) *Nature 416*, 279.
44. Vasella, A., Davies, G. J., and Bohm, M. (2002) *Curr. Opin. Chem. Biol. 6*, 619.

BI034329J